Respirable Coal Dust Particles Modify Cytochrome P4501A1 (CYP1A1) Expression in Rat Alveolar Cells

Mohamed M. Ghanem, Dale Porter, Lori A. Battelli, Val Vallyathan, Michael L. Kashon, Jane Y. Ma, Mark W. Barger, Joginder Nath, Vincent Castranova, and Ann F. Hubbs

Health Effects Laboratory Division, National Institute for Occupational Safety and Health, Centers for Disease Control and Prevention, Morgantown; and Genetics and Developmental Biology Program, West Virginia University, Morgantown, West Virginia

Cytochrome P4501A1 (CYP1A1) metabolizes polycyclic aromatic hydrocarbons in cigarette smoke to DNA-binding reactive intermediates associated with carcinogenesis. Epidemiologic studies indicate that the majority of coal miners are smokers but have a lower risk of lung cancer than other smokers. We hypothesized that coal dust (CD) exposure modifies pulmonary carcinogenesis by altering CYP1A1 induction. Therefore, male Sprague Dawley rats were intratracheally instilled with 2.5, 10, 20, or 40 mg CD/rat or vehicle (saline); and 11 d later, pulmonary CYP1A1 was induced by intraperitoneal injection of β-naphthoflavone (BNF; 50 mg/kg). Fourteen days after CD exposure, CYP1A1 protein and activity were measured by Western blot and 7-ethoxyresorufin-O-deethylase activity, respectively. CYP1A1 and the alveolar type II markers, cytokeratins 8/18, were localized and quantified in lung sections by dual immunofluorescence with morphometry. The area of CYP1A1 expression in alveolar septa and alveolar type II cells in response to BNF was reduced by exposure to 20 or 40 mg CD compared with BNF alone. CD exposure significantly inhibited BNF-induced 7-ethoxyresorufin-O-deethylase activity in a dose-responsive manner. By Western blot, induction of CYP1A1 protein by BNF was significantly reduced by 40 mg CD compared with BNF alone. These findings indicate that CD decreases BNF-induced CYP1A1 protein expression and activity in the lung.

Studies of CYPs have recently received great interest because these enzymes play critical roles in the metabolism of drugs, carcinogens, dietary xenobiotics and steroid hormones (1). The CYP proteins are heme-containing proteins, which are members of a gene superfamily that contains almost 1,000 members in species ranging from bacteria to plants and animals (2). CYP1A1 has garnered particular interest because of its involvement in the conversion of organic compounds, like polycyclic aromatic hydrocarbons (PAHs) in cigarette smoke, into carcinogenic intermediate species (3–5) that can initiate lung cancer development. Moreover, the expression of CYP1A1 can be induced at the transcriptional level by its substrates. The transcriptional regulation of the CYP1A1 gene by PAHs is mediated through ligand-dependent activation of the aryl hydrocarbon receptor (AhR), which translocates to the nucleus upon activation, dimerizes to the aryl hydrocarbon receptor nuclear translocator (Arnt) protein and binds to the xenobiotic responsive element (XRE) in the regulatory region of the CYP1A1 gene (6, 7).

Coal is a fossil fuel mined all over the world. Coal dust (CD) generated during underground coal mining results in significant respiratory exposure of coal miners. In addition to the carbon, which is the main component, coal also contains oxygen, nitrogen, hydrogen, and trace elements, and several inorganic minerals. The trace elements may include copper, nickel, cadmium, boron, antimony, iron, lead, and zinc (8). Some of these trace elements can be cytotoxic and carcinogenic in experimental models (9). Mineral contaminants include quartz, kaolin, mica, pyrite, and calcite. Coal dust inhalation is associated with development of a respiratory disease of coal miners called coal workers' pneumoconiosis (CWP). CWP is categorized according to severity into simple and complicated CWP. In the simple form, black dust macules appear and consist of dust-laden macrophages concentrated near respiratory bronchioles. In complicated CWP, also described as progressive massive fibrosis (PMF), the nodules are larger (exceeding 1 cm diameter) and more numerous. These nodules contain increased amounts of collagen, CD, and inflammatory cells (9).

CD exposure in miners with CWP tends to be very high and can include doses which put the lung in overload. For example, in one autopsy study, retired U.S. coal miners had a total dust burden of 13.5 ± 8.0 or 16.4 ± 8.5 g per lung (mean ± SD) for smokers and nonsmokers, respectively (10). In U.K. miners with PMF mining high rank coal (high carbon content), the mean lung dust burden was 26.4 g per lung (11). Assuming an average lung weight of 1,000 g, this represents a retained lung burden of 13.5 to 26.5 mg dust/g lung wet weight. Pulmonary inflammation is associated with coal mine and silica dust exposure in coal miners (12, 13).

Epidemiologic studies indicate that lung cancer in coal miners occurs less frequently than in the general population after adjustment for age and smoking (14, 15). Instead, CD exposure is associated with lung scarring (pulmonary fibrosis), inflammation, and accumulation of particles in dust-laden alveolar macrophages (9). Most of the studies of lung cancer in coal miners are difficult to interpret because of epidemiologic limitations and have not been adequately controlled for smoking. Because increased pulmonary CYP1A1 activity is associated with increased benzo[a]pyrene DNA adducts and risk of lung cancer from cigarette smoking (16), alterations in CYP1A1 from exposures in coal mining could affect the lung cancer risk.

Acid-washed but not aged respirable silica dust increases the activity of CYP1A1 in the lung of exposed rats (17, 18). Conversely, inhalation of CD or diesel exhaust (2 mg/m^3) for 1 yr does not affect CYP1A1-dependent benzo(a)pyrene hydroxy-

(*Received in original form November 24, 2003 and in revised form March 20, 2004*)

Address correspondence to: Dr. Ann F. Hubbs, Pathology and Physiology Research Branch, Health Effects Laboratory Division, National Institute for Occupational Safety and Health, Centers for Disease Control and Prevention, 1095 Willowdale Rd., Morgantown, WV 26505. E-mail: Ahubbs@cdc.gov

Abbreviations: aryl hydrocarbon receptor, AhR; alveolar macrophages, AM; aryl hydrocarbon receptor nuclear translocator, Arnt; alveolar type II cells, AT-II; bronchoalveolar lavage, BAL; BAL fluid, BALF; bicinchoninic acid, BCA; β-naphthoflavone, BNF; coal mine dust, CD; coal workers' pneumoconiosis, CWP; cytochrome P4501A1, CYP1A1; cytochrome P4502B1, CYP2B1; enhanced chemiluminescence, ECL; 7-ethoxyresorufin-*O*-deethylase, EROD; fluorescein isothiocyanate, FITC; immunoglobulin G, IgG; lactate dehydrogenase, LDH; neutral buffered formalin, NBF; proximal alveolar, PA; polycyclic aromatic hydrocarbon, PAH; phosphate-buffered saline, PBS; progressive massive fibrosis, PMF; polymorphonuclear leukocytes, PMN; 7-pentoxyresorufin-*O*-deethylase, PROD; random alveolar, RA; tris-buffered saline, TBS; xenobiotic responsive element, XRE.

Am. J. Respir. Cell Mol. Biol. Vol. 31, pp. 171–183, 2004
Originally Published in Press as DOI: 10.1165/rcmb.2003-0425OC on April 8, 2004
Internet address: www.atsjournals.org

lase activity (19). Similarly, intratracheally instilled carbon black particles have no effect on CYP1A1 protein or activity, although CYP2B1 protein and activity are decreased by this exposure (20). Consistent with that, preliminary experiments from our laboratory with respirable CD indicated that intratracheal instillation of 2.5 or 10 mg did not significantly alter CYP1A1 activity in the rat lung. CYP1A1 exerts its major known influence on pulmonary carcinogenesis by activating procarcinogenic PAHs, which are themselves substrates for, and powerful inducers of, CYP1A1. Thus, it is individuals exposed to PAHs who have induced CYP1A1, who will be most affected by modifying CYP1A1 activity. Induction of CYP1A1 is downregulated by inflammation both *in vitro* and *in vivo* (7, 21, 22). However, the influence of CD exposure on CYP1A1 induction has not been investigated.

Recent studies from our laboratory suggest that exposure to crystalline silica decreases the activity of the CYP1A1-dependent enzymatic process, 7-ethoxyresorufin-*O*-dethylase (EROD), in rat lungs exposed to a potent CYP1A1 inducer, β-naphthoflavone (23). Silicosis in rats is also associated with the appearance of a new population of alveolar epithelial cells without detectable expression of CYP1A1 or CYP2B1, even after exposure to inducers of CYP1A1 (23, 24). If other fibrogenic inhaled particulates, such as CD, also reduce the inducible activity of carcinogen-activating CYP1A1-dependent enzymatic processes, the expected result would be a reduction in the lung cancer attributable to chemical carcinogens activated by CYP1A1, such as the PAHs in cigarette smoke. Therefore, we investigated the effect of respirable CD on the metabolism of chemical carcinogens in lungs of rats. These studies will help determine if the effect of silica on CYP1A1 is a unique feature of silica dust or is a characteristic of pulmonary exposure to other respirable particles, which cause alveolar epithelial cell hypertrophy and hyperplasia, and pulmonary inflammation, such as CD.

For this purpose, we designed a dose–response experiment in rats to investigate the dose-dependent effect of CD on the inhibition of EROD. We intraperitoneally injected β-naphthoflavone (BNF), a model PAH, as a potent and specific CYP1A1 inducer (25). The study used the morphometric analysis of immunofluorescent-stained tissue to investigate the effect of CD on the inducible expression of CYP1A1 in the peripheral lung. We also determined the CYP1A1-dependent enzymatic activity, (EROD), in lung microsomes. Lungs from the same rats were microscopically examined to determine histopathologic alterations associated with changes in cell specific protein expression. Bronchoalveolar lavage (BAL) was performed on a separate group of rats to quantify pulmonary inflammation, cytotoxicity, and protein leakage. The amount of CYP1A1 protein in the lung microsomes of control and exposed rats was determined by Western blot analysis, using polyclonal rabbit anti-rat CYP1A1 antibodies. To our knowledge, this study demonstrates for the first time that CD exposure inhibits PAH-induced CYP1A1-dependent enzymatic activity in a dose-responsive fashion. This suppression was also observed in pulmonary alveolar septa of CD exposed rats by immunofluorescent-staining of lung sections. In addition, the amount of PAH-induced CYP1A1 detected by Western blot in lung microsomes was also diminished by exposure to CD. CD exposure and reduced CYP1A1 induction and CYP2B1 activity was also associated with alveolitis, albumin leakage and cytotoxicity, and alveolar epithelial cell hypertrophy and hyperplasia.

Materials and Methods

Animals

The experimental protocol was reviewed and approved by the Institution Animal Care and Use Committee. Male Sprague-Dawley rats (HLA: [SD]CVF) (~ 220–270 g) were purchased from Hilltop Labs (Scottdale, PA). Upon arrival, the rats were kept in an AAALAC-approved barrier animal facility at NIOSH. Food and water were supplied *ad libitum.* Rats were housed in ventilated shoebox cages on autoclaved hardwood (Beta-Chip; Northeastern Products, Inc., Warrensburg, NY) and cellulose (ALPHA-dri; Shepherd Specialty Papers, Watertown, TN) bedding in HEPA filtered, ventilated cage racks (Thoren Caging Systems, Inc., Hazleton, PA). Rats were allowed to acclimatize in their cages for at least 7 d before the experiment.

Experimental Design

CD exposures were designed to produce a broad range of lung-deposited CD concentrations per gram of lung tissue, with the exposures bracketing exposures of miners with CWP in autopsy studies (~ 10–25 mg CD/g lung wet weight) (10, 11). By using a research randomizer program (www.randomizer.org), rats were randomized into five groups of four rats each. Each group was intratracheally instilled with 0, 2.5, 10, 20, or 40 mg CD/rat (~ 0, 1, 4, 8, and 16 mg/100 g BW; and ~ 0, 1.7, 6.7, 13.3, or 26.7 mg CD/g lung wet weight for a 1.5 g rat lung) suspended in sterile saline. Eleven days later, rats were injected intraperitoneally with the CYP1A1 inducer BNF (50 mg/kg BW) suspended in filtered corn oil. Three days after BNF injection, rats were killed and the right lung lobes were homogenized for collection of the lung microsomes, whereas the left lungs were inflated with 10% neutral buffered formalin for histopathology.

CD Particles

CD was obtained from the Pittsburgh coal seam and size fractionated and characterized as previously described (26). Briefly, the CD particles were fractionated by size using a Donaldson particle classifier, and size was further characterized by an aerodynamic particle sizer (TSI Model APS 3300; TSI Inc., Shoreview, MN). The surface area was determined by nitrogen adsorption and particles were further characterized using scanning electron microscopy with energy dispersive X-ray analysis. The mass median aerodynamic diameter was 3.4 μ, 98.9% of the particles were < 5 μ in diameter, with 17.9% of the particles < 1 μ in diameter. The surface area was 7.4 m^2/g. The particles contained 0.34% total iron, of which 0.119% was surface iron. By number percentage, 2.3% of the particles were silica. The particles were weighed, placed in a scintillation vial, covered with foil, and heat sterilized in an oven at 160°C for 2 h. CD suspensions were prepared from heat-sterilized samples using nonpyrogenic sterile saline (Abbott Laboratories, North Chicago, IL).

Intratracheal Instillation

The CD particles were suspended in sterile saline at a concentration of 8.3, 33.3, 66.6, and 133.3 mg/ml. Rats received either 0.3 ml of this suspension (~ 2.5, 10, 20, and 40 mg/rat) or equivalent dose of sterile saline (vehicle). The rats were anesthetized by intraperitoneal injection of sodium methohexital (Brevital; Eli Lilly, Indianapolis, IN) and were intratracheally instilled, using a 20-gauge, 4-inch ball-tipped animal feeding needle as previously described (27). Because the technical expertise of the instiller is critical for reproducible intratracheal instillation (28), all instillations were performed by one of the researchers (M.W.B.) with more than 10 yr of experience performing intratracheal instillations. Because CD is black, distribution of CD to both the left and right lung was assured by gross examination at necropsy.

BNF Preparation

Solutions of 5% (50 mg/ml) BNF (Sigma-Aldrich Co., St. Louis, MO) in corn oil were prepared 1 d before intraperitoneal injection. Before use, the corn oil was filtered with nonpyrogenic Acrodisc 25 mm syringe filter (0.2 μm diameter pore) (Pall Gelman Sciences, Ann Arbor, MI) to assure sterility. The solution suspension was vortexed until the particles were evenly suspended and then sonicated in Ultronics sonicator (Mahwa, NJ) for 15 min before injection. BNF solutions were injected once, intraperitoneally, at a dose of 50 mg/kg 3 d before killing.

Killing

Rats were killed by intraperitoneal injection of 0.5 ml 26% sodium pentobarbital (Sleepaway; Fort Dodge Animal Health, Fort Dodge, IA) 2 wk after CD exposure.

Necropsy

The lungs and attached organs, including tracheobronchial lymph node, thymus, heart, aorta, and esophagus, were removed. The right lung lobes were collected and weighed at necropsy for microsomal preparation, whereas the left lung lobe was inflated with 3 cc of 10% neutral buffered formalin (NBF). Tracheobronchial lymph nodes, liver, spleen, and right and left kidneys were also fixed in 10% NBF. Fixed tissues were trimmed the same day, routinely processed in a tissue processor, and embedded in paraffin the following morning. Tissue sections of left lung were stained with hemotoxylin and eosin (H&E). Additional 5-μm sections were used for immunofluorescence.

Separate rats were designated for BAL studies which are described below.

Microsomal Preparation

Lung microsomes were prepared for determination of EROD activity as an indicator of CYP1A1-dependent enzymatic activity, whereas 7-pentoxyresorufin-*O*-deethylase (PROD) activity was determined as an indicator of the CYP2B1-dependent enzymatic activity. Lung microsomes were also used for Western blot analysis of CYP1A1 and CYP2B1 proteins. Microsomes were prepared as previously described (29, 30). At the necropsy, the right lung lobes were weighed and chopped four times with a McIlwain tissue chopper (Mickle Engineering Co., Gomshall, Surrey, UK) set at slice thickness of 0.5 mm. Then, the chopped lung tissues were suspended in ice-cold incubation medium (145 mM KCl, 1.9 mM KH_2PO_4, 8.1 mM K_2HPO_4, 30 mM Tris-HCl, and 3 mM $MgCl_2$; pH 7.4) at a ratio of 1 g lung to 4 ml incubation medium. The suspended solution was homogenized using a Teflon-glass Potter-Elvejhem homogenizer (Emerson, NJ) through 16 complete passes. The cell nuclei and debris were removed by centrifugation of the homogenate at 2,500 rpm for 10 min in a Sorvall Model RC2-B refrigerated centrifuge (Ivan Sorvall Co., Norwalk, CT). Mitochondria were slowly deposited by three sequential centrifugations for 20 min each at 5,000, 9,000, and 13,000 rpm to reduce the mitochondrial contamination of the microsomes. The resulting supernatant was ultracentrifuged at 40,000 rpm for 75 min in a Beckman Model L5–50 ultracentrifuge (Beckman Instruments, Palo Alto, CA) to obtain the microsomal fraction. The pellet was resuspended in the incubation medium at a ratio equal to the original lung weight (i.e., 1 g lung/1 ml medium) and frozen at −80°C until assayed.

Determination of the Total Lung Proteins

The protein content of lung microsomes was measured by the bicinchoninic acid method as previously described (30, 31) using a bicinchoninic acid protein assay kit (Pierce, Rockford, IL) in a spectra Max 250 spectrophotometer (Molecular Devices Corporation, Sunnyvale, CA). Bovine serum albumin was used as the standard.

Measurement of EROD and PROD Activities

EROD and PROD activities were measured as previously described (30, 32) using a luminescence spectrometer, model LS-50 (Perkin-Elmer, Norwalk, CT). A 10-μM concentration of 7-ethoxyresorufin (Sigma-Aldrich) solution, prepared from 2.35 μg 7-ethoxyresorufin in 1 ml DMSO, was used to obtain the standard curve for each run. EROD and PROD activities were expressed as picomoles of the produced resorufin per minute per milligram of microsomal protein (pmol/min/mg protein).

Western Blot Analysis

Western blot analysis of lung microsomes was conducted as previously described (30). Each gel received 75 μg of microsomal protein for CYP1A1 and 20 μg for CYP2B1, that were subjected to sodium dodecyl sulfate gel electrophoresis for 90 min at 120 V followed by blotting to a nitrocellulose membrane for 90 min at 25 V. Blocking of nonspecific binding was made by incubating the membrane with a solution of 1% dry milk in tris-buffered saline (TBS) for 1 h at room temperature with rocking. The nitrocellulose membrane was probed, using a polyclonal rabbit anti-rat CYP1A1 antibody (Xenotech, Kansas City, KS) or a monoclonal mouse anti-rat CYP2B1 antibody (Xenotech) at 4°C overnight. The membranes were then incubated for 1 h at room temperature with a goat anti-rabbit antibody (Santa Cruz Biotech, Inc., Santa Cruz, CA) for CYP1A1 or goat anti-mouse antibody (Santa Cruz Biotech) for CYP2B1. For the positive controls, liver microsomes of BNF-treated rats (Xenotech) were used for CYP1A1 or liver microsomes of phenobarbital-treated rats (Amersham, Piscataway, NJ) for CYP2B1. The CYP1A1 and CYP2B1 proteins were detected by an enhanced chemiluminescence (ECL) reagent kit (Amersham). The X-ray films (Fuji Photo Film Co. Ltd., Tokyo, Japan) containing protein bands were scanned by the Eagle Eye II scanner (Stratagene, La Jolla, CA) with Eagle Sight software. The scanned images were quantified by ImageQuant software version 5.1 (Molecular Dynamics, Sunnyvale, CA). The quantification of Western blots by this software calculates the volume under the surface area created by a 3-D plot of the pixel locations and pixel intensities. The data were expressed as a percentage of the CYP1A1 or CYP2B1 positive controls.

Dual Immunofluorescence Technique

Paraffin-embedded, formalin-fixed sections from the left lung lobe were used for immunofluorescent detection of CYP1A1 and cytokeratins 8/18, which are cytoskeletal proteins used as markers of alveolar type II cells (AT-II) (33). Briefly, immunofluorescence was a two-day procedure. On the first day, the slides were first heated in the oven at 60°C for 10 to 20 min. The slides were deparaffinized and rehydrated in xylene in three sequential 6-min immersions, a 3-min immersion in 100% alcohol, 3 min in 90% alcohol, 3 min in 80% alcohol, and 5 min in distilled water. The antigenicity of hidden epitopes was retrieved using 0.01 M EDTA (Fisher Scientific, Fair Lawn, NJ), pH 8, in a microwave heating procedure. Specifically, slides in the EDTA solution were heated for 1 min and 45 s in the microwave (Kenmore, Model #565.8962690; Sears, Roebuck and Co., Chicago, IL) on high and then for 6 min on defrost. EDTA solution was then added to replenish the solution which had been evaporated, and the slides were reheated for six additional minutes on defrost. To avoid the nonspecific binding of the primary antibodies, the slides were blocked with 5% bovine serum albumin in phosphate-buffered saline (PBS, IgG free; Sigma-Aldrich Co.) for 10 min at room temperature. Then the slides were rinsed with distilled water and blocked with 5% pig serum in PBS (Biomeda Corporation, Foster City, CA) for 10 min at room temperature. The slides were then rinsed with distilled water and primary antibodies were applied. We used a polyclonal guinea pig anti-cytokeratins 8/18 antibody (Research Diagnostics Inc., Flanders, NJ) for staining of cytokeratins 8/18 at a 1:50 dilution in PBS. For CYP1A1 staining, a polyclonal, affinity-purified, highly cross-absorbed rabbit anti-rat CYP1A1 antibody (Xenotech) was used at a 1:5 dilution. Both primary antibodies were applied by utilizing the capillarity generated between each pair of slides in a microprobe holder (Fisher Scientific). The slides were kept at room temperature overnight during which time the primary antibodies were allowed to bind to the antigen (CYP1A1 or cytokeratins 8/18). On the second day, the slides were incubated in the oven at 37°C for 2 h, after which they were thoroughly rinsed with distilled water, and the secondary antibodies were dropped onto the slides. An FITC-labeled, donkey anti–guinea pig IgG (Research Diagnostics Inc.) was used to detect cytokeratins 8/18 at a 1:50 dilution with PBS. For CYP1A1 detection, Alexa 594–conjugated goat anti-rabbit antibody (Molecular Probes, Eugene, OR) was applied at a dilution of 1:20 with PBS. The secondary antibodies were allowed to bind to the primary antibodies for 2 h in the dark. For the negative control, the primary antibodies were omitted and replaced by rabbit serum. Slides were rinsed with distilled water, cover slips were applied using gel mount (Biomeda Corp.); and the slides were allowed to dry for 2 h.

Slides were visualized on an Olympus fluorescent photomicroscope (Olympus AX70; Olympus American Inc., Lake Success, NY) using two filters: (*i*) a green cube (460–500 nm excitation) and (*ii*) a red cube (532.5–587.5 nm excitation). Ten microscopic fields of the alveolar regions were captured by a researcher blinded to the exposure status using a digital camera (Quantix Photometrics; Roper Scientific Inc., Trenton, NJ). Each field was captured as visualized green, red, and dual fluorescence. For each slide, five microscopic fields were captured from proximal alveolar (PA) regions where most of the dust particles tend to accumulate (34). Another five fields were obtained from alveoli that were not located near visible alveolar ducts, and these were designated as random alveolar (RA) regions. Selecting those two areas as-

sured sampling of the PA regions representative of the site of CD particle deposition as well as RA regions, which are less likely to be sites of particle deposition. Five microscopic fields were also captured as digital images from the terminal bronchiolar region to count the number of CYP1A1-positive bronchiolar epithelial cells. The digital camera settings for contrast, brightness, and γ were held constant for all slides. The staining was described as being specific due to the absence of background staining, distinct cellular localization of CYP1A1 and cytokeratins 8/18, and absence of the staining in the negative control slides where rabbit serum was applied instead of the primary antibodies.

Quantification of CYP1A1 and Cytokeratins 8/18 by Morphometric Analysis

The lung area occupied by red fluorescence (representing CYP1A1 expression), green fluorescence (representing cytokeratins 8/18, which are cytoskeletal proteins highly expressed in primitive epithelia such as the cuboidal AT-II [33]), and colocalized (concomitantly occurring) red and green fluorescence were quantified using commercial morphometry software (Metamorph Universal Image Corp., Downingtown, PA). The area of CYP1A1 colocalized with cytokeratins 8/18 in AT-II was obtained by the following formula: $C = R \times T$, where C stands for the area of CYP1A1 that co-expressed (colocalized) with cytokeratins 8/18 in AT-II, R stands for the percent of CYP1A1 expressed in AT-II measured by the Metamorph software, and T stands for the total CYP1A1 area expressed in the whole alveolar septum (including AT-II and alveolar non-type II cells) measured by the Metamorph software.

Moreover, the proportional CYP1A1 expression in AT-II, which is the relative area of CYP1A1 to cytokeratins 8/18 expression, was calculated from the following formula:

$$P = \frac{R \times T}{G},$$

where R and T are as defined above and G is the total green area of cytokeratins 8/18 expressed in AT-II cells. P is the proportional CYP1A1 expression within areas occupied by the AT-II marker, and adjusts for increases associated with AT-II hyperplasia.

By this method, we were able to analyze the expression pattern in AT-II. Moreover, the hyperplasia of AT-II was also determined by measuring the area containing the FITC expression (green area), which represents the expression of cytoskeletal proteins 8/18 by AT-II. The threshold ranges for red and green colors were held constant during morphometric analysis of all images.

Histopathology

Slides were interpreted by a board-certified veterinary pathologist blinded to the exposure status of the individual slides. Changes assessed in each slide included: AT-II hyperplasia and hypertrophy, alveolitis (inflammation), and hyperplasia of bronchus-associated lymph tissue. Histopathologic changes were scored for severity and distribution from zero to five as previously described (35). Briefly, severity was scored as none (0), minimal (1), mild (2), moderate (3), marked (4), or severe (5). Distribution was scored as none (0), focal (1), locally extensive (2), multifocal (3), multifocal and coalescent (4), or diffuse (5). The pathology score was the sum of the severity and distribution score.

BAL and Cell Differentials

Lungs were lavaged and cells collected as previously described (36). To assess pulmonary inflammation, cell counts of alveolar macrophages (AM) and polymophonuclear leukocytes (PMN) were obtained using a Coulter Multisizer II (Coulter Electronics, Hialeah, FL) as previously described (37).

BAL Fluid Albumin Concentration

BAL fluid (BALF) albumin concentrations were determined as an indicator of the integrity of the blood-pulmonary barrier. BALF albumin was measured colorimetrically at 628 nm based on albumin binding to bromcresol green (38) using a commercial assay kit (Albumin BCG diagnostic kit; Sigma Chemical Co.) and a COBAS MIRA Analyzer (Roche Diagnostics, Indianapolis, IN).

BALF Lactate Dehydrogenase Activity

BALF lactate dehydrogenase (LDH) activities were determined as a marker of cytotoxicity, and were determined by monitoring the LDH catalyzed oxidation of lactate to pyruvate coupled with the reduction of AAD^+ at 340 nm (39) using a commercial assay kit (Roche Diagnostics) and a COBAS MIRA Analyzer (Roche Diagnostics).

Zymosan-Stimulated AM Chemiluminescence

AM chemiluminescence was determined as an indicator of reactive oxygen and nitrogen species production by AM. The use of unopsonized zymosan in the chemiluminescence assay allows only AM chemiluminescence to be measured, because unopsonized zymosan stimulates AM chemiluminescence (40) but not PMN chemiluminescence (41, 42). The assay was conducted in a total volume of 0.50 ml HEPES buffer. Resting AM chemiluminescence was determined by incubating 1.0×10^6 AM/ml at 37°C for 20 min, followed by the addition of 5-amino-2,3-dihydro-1,4-phthalazinedione (luminol) to a final concentration of 0.08 μg/ml followed by the measurement of chemiluminescence. To determine zymosan-stimulated chemiluminescence, unopsonized zymosan was added to a final concentration of 2 mg/ml immediately before the measurement of chemiluminescence. All chemiluminescence measurements were made with an automated luminometer (LB 953; Berthold Autolumat, Gaithersburg, MD) at 390–620 nm for 15 min. The integral of counts per minute versus time was calculated. Zymosan-stimulated (total) chemiluminescence was calculated as the cpm in the zymosan-stimulated sample minus the cpm in the resting sample. 1400W (N-(3-aminomethyl)benzyl)acetamidine•HCl), an inhibitor of nitric oxide synthase, was used to determine the component of zymosan-stimulated (total) chemiluminescence that is attributable to reactive nitrogen species. 1400W-sensitive chemiluminescence was determined by subtracting the zymosan-stimulated chemiluminescence from cells pre-incubated with 1 mM 1400W from the zymosan-stimulated (total) chemiluminescence from AM without 1400W.

Statistical Analyses

The dose responsive effects of CD instillation on EROD, PROD, and Western blot for CYP1A1 and CYP2B1 were assessed, using linear regression analysis. Pairwise comparisons of each dose to the control group were analyzed, using one-way ANOVA followed by Dunnett's test. AT-II hyperplasia and hypertrophy based on immunofluorescence were analyzed, using one-way ANOVA followed by Dunnett's test to compare each dose to the control group. Pathology scores were analyzed using the nonparametric Kruskal-Wallis test followed by the Wilcoxon Rank-sum test for pairwise comparisons. All differences were considered statistically significant at $P < 0.05$.

Results

Effect of CD Exposure on EROD and PROD

The IT instillation of CD suppressed the BNF-induced CYP1A1-dependent enzymatic activity (EROD) in a dose-dependent fashion ($r^2 = 0.399$, $P = 0.0028$) (Figure 1A). Rats exposed to 20 or 40 mg CD/rat had a significant lower BNF-induced EROD activity than those exposed to saline ($P = 0.036$). Similarly, CYB2B1-dependent enzymatic activity (PROD), the major CYP isoform in rat lungs, showed a dose-dependent reduction by CD exposure using linear regression ($r^2 = 0.458$, $P = 0.001$). BNF-treated PROD was significantly reduced in rats exposed to 20 and 40 mg CD/rat compared with saline controls ($P = 0.017$) (Figure 1B).

Western Blot Analysis

CYP1A1. A representative Western blot of CYP1A1 is shown in Figure 2A. The results are expressed as the percentage of the CYP1A1 positive control. The amount of BNF-induced CYP1A1 quantified by Western blot after CD exposure was less than in control rats. Groups treated with the highest dose of CD (40 mg/rat) showed a significant reduction of BNF-induced CYP1A1 protein compared with control ($P = 0.03$) (Figures 2A and 2B).

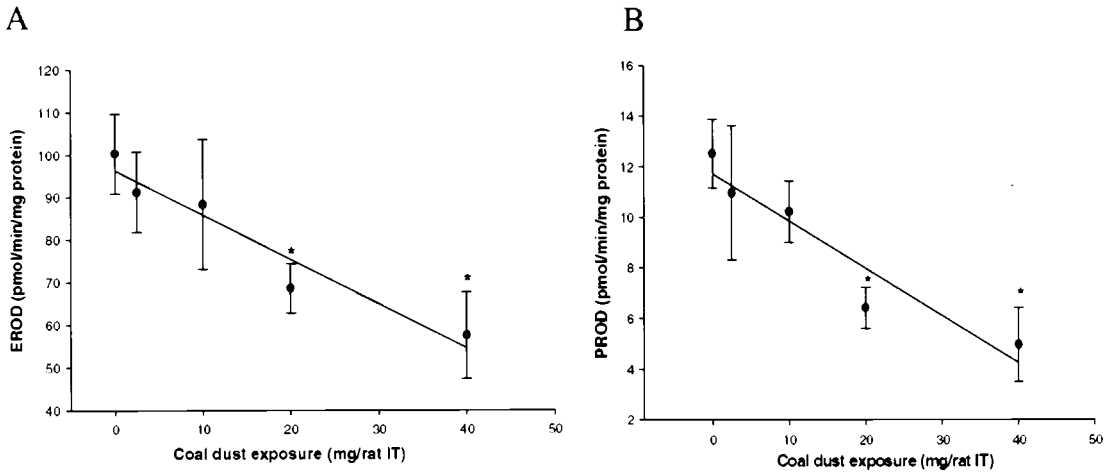

Figure 1. Effect of CD exposure on EROD and PROD. (*A*) BNF-induced CYP1A1-dependent enzymatic activity (EROD) was suppressed in a dose-dependent fashion by intratracheal exposure of rats to 0, 2.5, 10, 20, or 40 mg CD. (*B*) CYP2B1-dependent enzymatic activity (PROD) was suppressed in a dose-dependent fashion by intratracheal exposure of rats to 0, 2.5, 10, 20, or 40 mg CD. EROD and PROD activities in response to BNF were significantly reduced at 20 and 40 mg/rat CD exposure with BNF compared with the control (saline/BNF). The linear regression best fit curves show the reduction of EROD and PROD activities with increasing CD exposure. Values are means ± SE, $n = 4$. *Significantly different from control at $P < 0.05$.

CYP2B1. The CYP2B1 protein, the major isoform of CYP subfamily in the rat lung, was measured in the lung microsomes. CYP2B1 is not inducible by BNF in rat lungs but can be induced in liver by phenobarbital. The amount of lung CYP2B1 detected by Western blot was not significantly affected in CD-exposed rats compared with control rats (Figures 2C and 2D). The results were expressed as the percentage of CYP2B1 in the positive control.

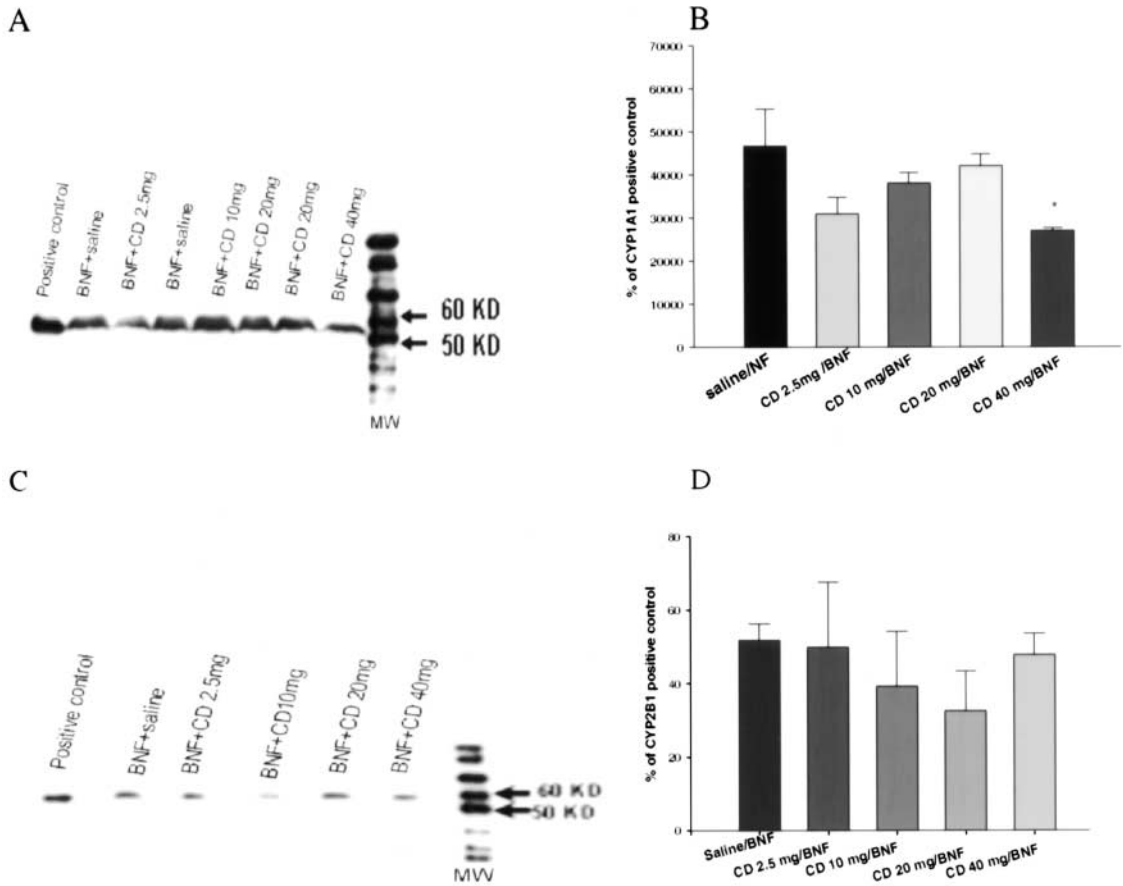

Figure 2. Effect of CD on CYP1A1 and CYP2B1 expression in rat lung as assessed by Western blot. Each lane received equal loading of microsomal protein (75 μg for CYP1A1 and 20 μg for CYP2B1). (A) A sample of Western blot showing significant repression of the BNF-induced CYP1A1 protein in lung microsomes by CD exposure ($P = 0.029$) at the highest dose of CD (40 mg/rat). (*B*) The data from multiple Western blots are expressed as the percentage of CYP1A1 positive control from quantification of four different samples from each exposure group. (*C*) Western blot of CYP2B1 protein is shown. The amount of lung CYP2B1 detected by Western blot was decreased, although not significantly, by CD exposure. (*D*) Four different samples for each treatment were quantified and the data expressed as a percentage of positive CYP2B1 control. The values represent means ± SE, $n = 4$. *Significantly different from control group at $P < 0.05$.

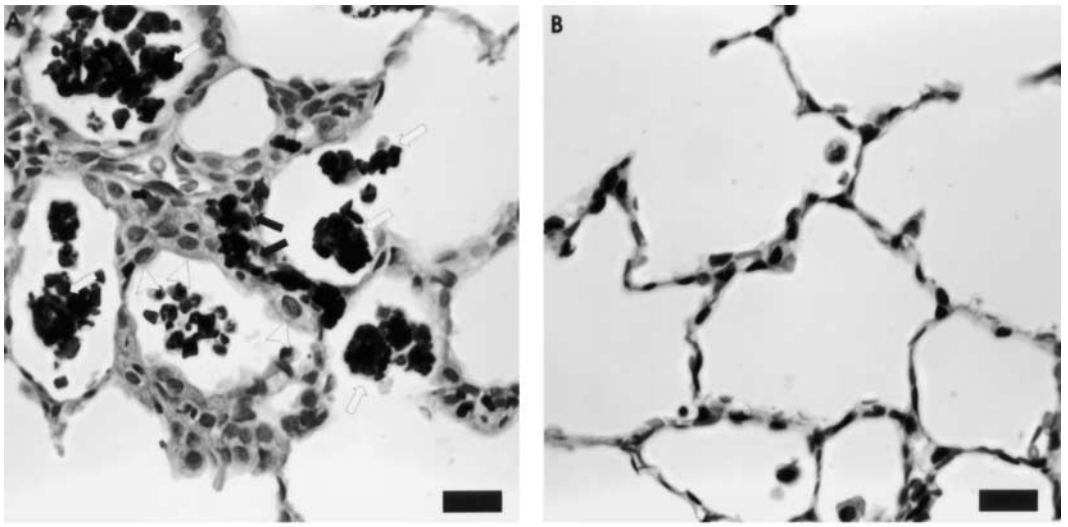

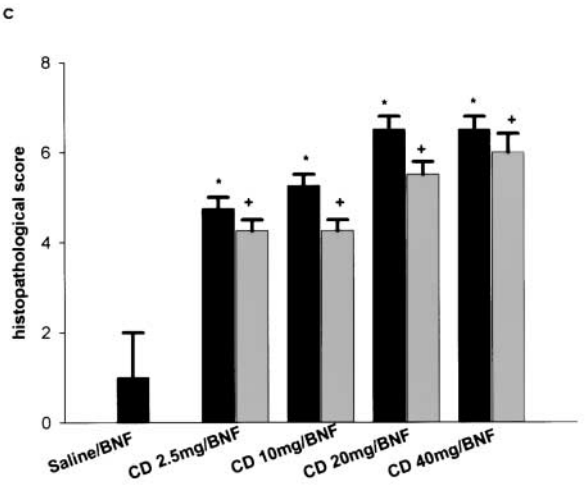

Figure 3. Histopathologic alterations in CD-exposed lungs. (*A*) Photomicrograph of a tissue section stained with H&E showing AT-II hyperplasia and hypertrophy (*arrowheads*). Dust-laden macrophages are within the alveolar spaces (*white arrows*) and interstitial tissues (*black arrows*). (*B*) Photomicrograph of tissue section of control stained with H&E showing absence of histopathologic changes. The *magnification bar* is 20 μm. (*C*) Histopathologic changes in rat lungs after intratracheal exposure to CD. Changes were scored for severity and distribution of alveolitis (*dark bars*) and AT-II hyperplasia (*light bars*) and hypertrophy. *Asterisk* indicates that alveolitis is significantly higher than control (saline/BNF) at $P < 0.05$. *Plus sign* indicates that AT-II hyperplasia and hypertrophy are significantly higher than control (saline/BNF) at $P < 0.05$. Values are means ± SE.

Gross Pathology

Multifocal gray foci were visible from the pleural surface of the CD-exposed rats, were present in all lung lobes, and were increasingly apparent with increasing exposures.

Effect of CD Exposure on Histopathologic Changes of Lung Alveolar and Tracheobronchial Region

AT-II hyperplasia (increased cell number) and hypertrophy (increased cell size), alveolitis (alveolar inflammation), and lymphoid hyperplasia of tracheobronchial lymph nodes were the major histopathologic changes identified in sections stained by H&E. Accumulation of dust-laden macrophages in the alveolar spaces was a noteworthy finding in CD-exposed alveoli (Figure 3A). Rats exposed to CD (2.5, 10, 20, and 40 mg/rat) showed significant hyperplasia and hypertrophy of AT-II (Figure 3A) compared with control ($P < 0.001$) in all treatment doses (Figure 3). In addition, alveolitis (alveolar inflammation) was significantly increased in rats exposed to 2.5, 10, 20, and 40mg/rat CD ($P = 0.01$, $P = 0.006$, $P = 0.002$, $P = 0.002$, respectively) (Figure 3C).

Results of Dual Immunofluorescence

The result of immunofluorescent changes indicate that CD exposure increases AT-II staining and decreased BNF-induced CYP1A1 staining of AT-II and non–AT-II in the alveolar septa of the proximal alveoli but not the random alveoli.

Pattern of CYP1A1 expression in the alveolar region of the lung. A specific pattern of rat CYP1A1 expression was observed in the alveolar region of the lung by immunofluorescence examination. In rats exposed to BNF alone (control rats), the CYP1A1 expression (*red-labeled area* in Figures 4B and 4C) was principally localized to the endothelium of the pulmonary vasculature and in cells of the alveolar septum. Statistically, areas of CYP1A1 expression were significantly smaller in AT-II than in other cells (non–AT-II) of the alveolar septum ($P = 0.003$) (Figures 4C and 4D).

Pattern of cytokeratins 8/18 expression in the alveolar region of the lung. The green fluorescent cytokeratins 8/18 were clearly expressed in the cytoplasm of cuboidal cells that were mainly localized on the corners of the alveolar septum (Figure 4A). These cells have the plump morphology characteristic of AT-II of the alveolar septa. No green fluorescence was visualized in the other types of cells of the alveolar septum, which were then designated as non–AT-II (Figure 4A).

Effect of CD on AT-II proliferation by immunofluorescent examination. The area of expression of cytoskeletal proteins (cytokeratins 8/18), which are highly expressed in the cytoplasm of AT-II was quantified morphometrically and expressed as square micrometers. In the PA regions, this area was significantly larger in rats exposed to 20 and 40 mg CD/rat and BNF than control (Figures 5A, 5B, and 6A), indicating hyperplasia and

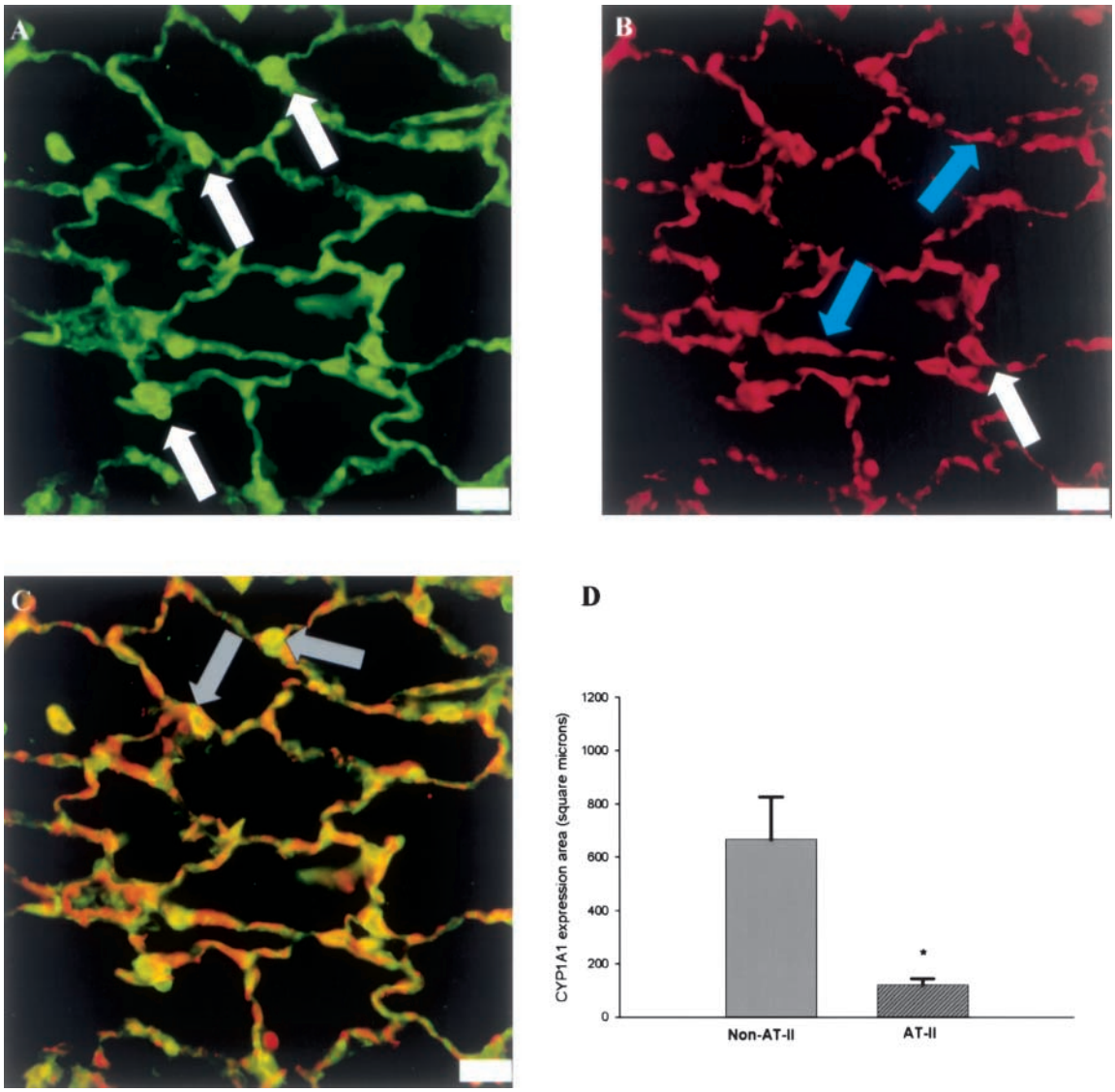

Figure 4. Immunofluorescent staining of pulmonary CYP1A1 and cytokeratins 8/18 of BNF-exposed rat alveoli. (*A*) The *green color* shown represents the staining of cytokeratins 8/18 expressed in AT-II, which appear as plump cells at the corners of the alveoli (*white arrows*). (*B*) The *red fluorescence* stains the areas of CYP1A1 expression in alveolar non-AT-II (*blue arrows*) and AT-II (*white arrows*). (*C*) The *green* and *red colors* were combined to visualize the concomitant localization (colocalization) of red CYP1A1 and green cytokeratins 8/18 within AT-II that gives rise to *yellow color* (*gray arrows*). The double labeling image shows that CYP1A1 expression in AT-II is less than expression in non–AT-II. (*D*) Morphometric analysis showing a significant reduction of the area of CYP1A1 expression in AT-II compared with non–AT-II. *Asterisk* indicates significant difference from CYP1A1 expression in alveolar non–AT-II at $P < 0.05$. *Reference bar* is 20 μm.

hypertrophy of AT-II ($P = 0.027$ and $P = 0.02$, respectively). By contrast, no significant AT-II hyperplasia and hypertrophy were detected in the random alveolar (RA) regions of CD-exposed rats compared with control (Figure 5C). Compared with RA regions, the area of cytokeratins 8/18 expression was significantly larger in the PA regions of rats exposed to 40 mg CD plus BNF (Figure 6A).

Effect of CD exposure on CYP1A1 expression by non–AT-II. **CYP1A1 expression by non–AT-II Cells in saline versus CD-exposed rats.** In PA regions. The area of expression of CYP1A1 (measured in square micrometers) by non–AT-II (all cells in the alveolar septum except for AT-II) of PA regions (regions of CD accumulation) was significantly lowered in groups exposed to 20 mg and 40 mg CD/rat and BNF compared with BNF control group ($P = 0.007$, $P = 0.008$, respectively) (Figure 6B). This was indicated by the reduction of the red-labeled area that is not co-expressed with green-labeled area (Figures 5A and 5B).

In RA regions. No significant change was detected in the area of CYP1A1 expression by non–AT-II of RA regions (regions of minimal particle aggregation) of groups exposed to CD and BNF compared with control group. This result was illustrated by morphometric quantification of CYP1A1 expression in non–AT-II, where none of the cytokeratins 8/18 were localized with CYP1A1 (Figures 5C and 6).

CYP1A1 expression by non–AT-II in PA regions versus RA regions of CD-exposed rats. CYP1A1 expression by non-AT-II was compared in 2 different alveolar regions, the PA versus RA regions. The area of CYP1A1 expression measured in non-AT-II cells of PA regions was significantly reduced compared with the RA region in rats exposed to 20 and 40 mg CD/rat and BNF ($P = 0.048$, $P = 0.022$, respectively) (Figure 6B).

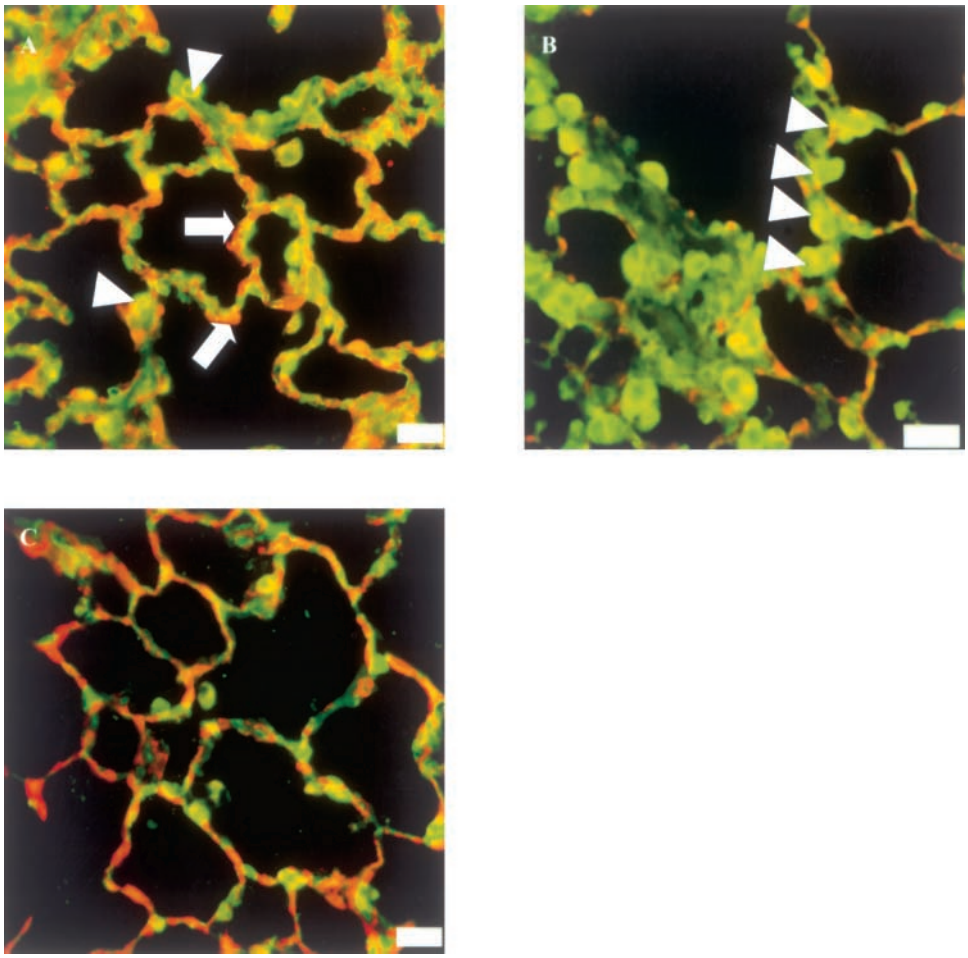

Figure 5. Representative immunofluorescence images of PA regions of BNF-treated rats and BNF and 40 mg CD–exposed rats showing reduction of CYP1A1 expression in AT-II and non–AT-II by CD exposure. (*A*) Dual immunofluorescence for CYP1A1 (*red*) and the AT-II markers, cytokeratins 8/18 (*green*) in the PA region. The CYP1A1 (*red fluorescence*) is expressed in the flattened non-AT-II (*arrows*), which constitute the majority of alveolar septum architecture and in AT-II (*arrowheads*, *yellow color* represents colocalization of *red* and *green fluorescence*), which are cuboidal cells mainly located at the corners of the alveoli. (*B*) the CYP1A1 expression in AT-II and non–AT-II was significantly reduced as shown by reduction of *red color* and *yellow color* in the alveolar septum. AT-II hyperplasia and hypertrophy (*arrowheads*) is also evident in the PA region of CD-exposed rats. (*C*) Representative immunofluorescence image of the RA regions of a rat exposed to BNF and the highest dose (40 mg/rat) of CD. No significant differences are apparent in the CYP1A1 expression between BNF and CD-exposed when compared with BNF-exposed rats. *Reference bar* is 20 μm.

Effect of CD exposure on CYP1A1 expression by AT-II. **CYP1A1 expression by AT-II in CD-exposed rats versus control in the PA regions.** Relative area (proportion) of CYP1A1 expression in AT-II. The relative area of red fluorescent CYP1A1 expression to the green fluorescent area of cytokeratins 8/18 expression was calculated by the formula described in Materials and Methods, and was designated as proportional CYP1A1 expression, which determines the amount of CYP1A1 expression within AT-II with correction for changes in AT-II number. The proportional CYP1A1 expression in AT-II of PA regions was significantly reduced in rats exposed to 20 mg (P = 0.005) and 40 mg (P = 0.003) CD and BNF compared with control (Figure 6C).

Area of CYP1A1 colocalized with cytokeratins 8/18 in AT-II. The expression of CYP1A1 in AT-II is visualized as a yellow fluorescence due to concomitant expression of the red-fluorescent CYP1A1 and green-fluorescent cytokeratins 8/18 (Figure 4). The expression (colocalization) of CYP1A1 in AT-II of the PA regions measured in μm^2 was not significantly lowered in rats exposed to 20 mg and 40 mg CD/rat plus BNF compared with control (Figure 6D). This was indicated by the reduction of the red areas that colocalized (co-expressed) with green areas in rats receiving higher exposures of CD (Figure 5B).

CYP1A1 expression by AT-II in CD-exposed rats versus control in RA regions. The expression of CYP1A1 in AT-II (either the colocalization or the proportional expression) was not significantly affected by CD exposure in RA regions (Figure 6C and 6D, respectively).

CYP1A1 expression by AT-II in PA regions versus RA regions of CD-exposed rats. The area of CYP1A1 expression measured in AT-II and the proportional CYP1A1 expression in AT-II showed no significant changes in PA regions when compared with RA regions in CD-exposed groups compared with BNF-exposed groups (Figures 6C and 6D, respectively).

Effect of CD exposure on CYP1A1 expression in the entire alveolar septum. The area of CYP1A1 expression was measured in alveolar septa as total red area, which represents the expression by all different types of cells in the septa. A significant reduction was detected with 20 and 40 mg CD/rat in PA regions (Figure 6E). However, there was no change observed in RA regions. In addition, in rats exposed to 20 and 40 mg of CD and BNF, CYP1A1 expression in PA regions was significantly less than in RA regions (Figure 6E).

Effect of CD on CYP1A1 expression by the nonciliated bronchiolar epithelial (Clara) cells. The number of the CYP1A1-positive nonciliated bronchiolar epithelial cells was counted per micrometer of the basement membrane. No significant change in the number of CYP1A1-positively stained cells was observed in BNF and CD-exposed rats compared with BNF-exposed rats (data not shown).

Effect of CD Exposure on BALF Analysis

CD-exposed rats had a dose-dependent increase in PMN (r^2 = 0.974, P = 0.002) (Figure 7A). The AM count was significantly increased in the BALF of all rats exposed to CD and BNF compared with rats treated with BNF alone (Figure 7B). AM

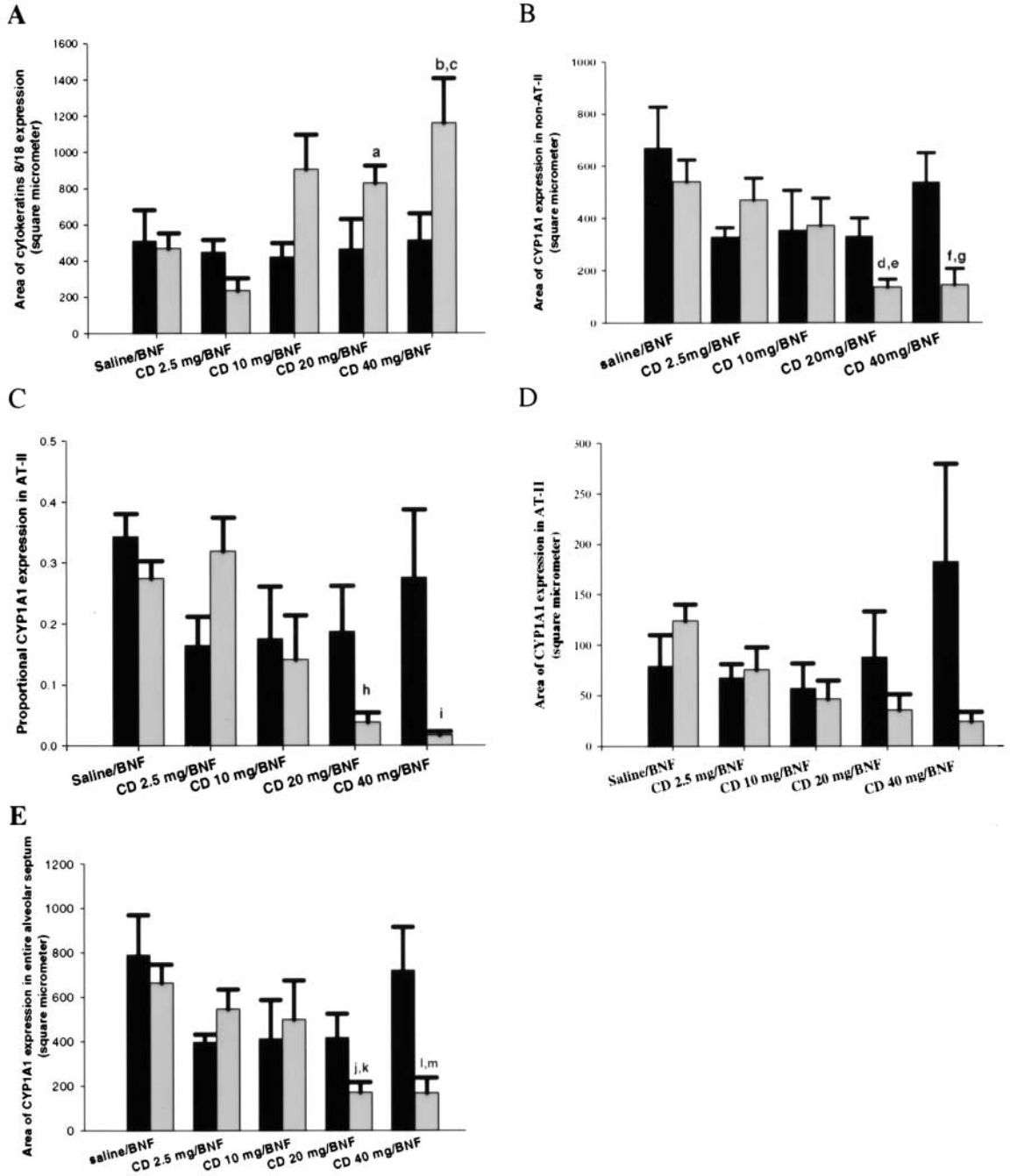

Figure 6. Morphometric quantification of area of cytokeratins 8/18 and CYP1A1 expression in rat alveoli. (*A*) The area of cytokeratins 8/18 expression in PA regions of rats exposed to 20 and 40 mg CD/rat and BNF is significantly increased compared with control (*letters a* and *b*, respectively). Compared with RA regions, the area of cytokeratins 8/18 expression in PA regions is significantly increased (*letter c*). (*B*) The area of CYP1A1 expression in non-AT-II is significantly decreased in PA regions of rats exposed to 20 and 40 mg CD/rat compared with control (*letters d* and *f*, respectively). Compared with RA regions, the area of CYP1A1 expression in the PA regions of rats exposed to 20 and 40 mg CD/rat and BNF is significantly decreased (*letters e* and *g*, respectively). (*C*) The proportional CYP1A1 expression in AT-II is significantly decreased in PA regions of rats exposed to 20 and 40 mg CD/rat and BNF compared with control (*letters h* and *i*, respectively). (*D*) The area of CYP1A1 expression colocalized in AT-II is not significantly affected by CD exposure. (*E*) The area of CYP1A1 expression in the entire alveolar septum of PA regions of rats exposed to 20 and 40 mg CD/rat is significantly decreased compared with control (*letters j* and *l*, respectively). Compared with RA regions, the area of CYP1A1 expression in the entire alveolar septum of PA regions of rats exposed to 20 and 40 mg CD/rat is significantly decreased (*letters k* and *m*, respectively). All values are means ± SE, $n = 4$. *Letters a–m* indicate significant difference at $P < 0.05$. *Dark bars*, RA regions; *light bars*, PA regions.

CL and NO-dependent CL were significantly increased in rats exposed to 40 mg CD and BNF compared with rats treated with BNF alone (Figures 7C and 7D, respectively). The intrapulmonary deposition of CD particles produced pulmonary cytotoxicity manifested by elevation of LDH activity in a dose-dependent fashion ($r^2 = 0.963$, $P = 0.003$) (Figure 7E). The blood barrier in the lung was also damaged in CD-exposed groups, as shown by elevation of BALF albumin, which was statistically significant after exposures to 20 and 40 mg/kg CD and BNF compared with BNF alone (Figure 7F).

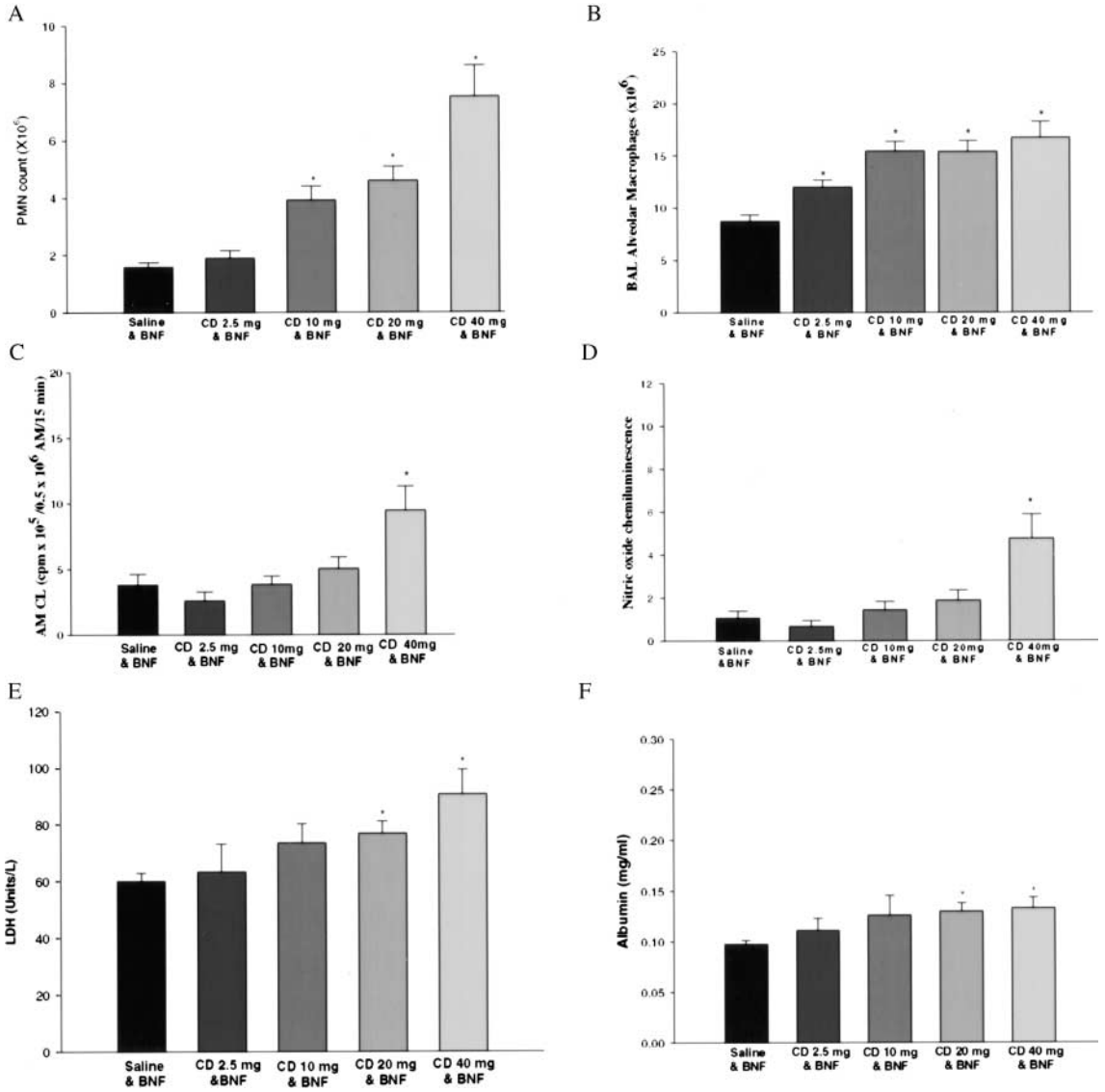

Figure 7. BAL findings indicate that combined exposure to CD and BNF resulted in pulmonary inflammation, enhanced alveolar macrophage chemiluminescence, LDH release consistent with cytotoxicity, and alterations in the blood barrier. (*A*) A significant PMN increase is shown in rats exposed to 10, 20, and 40 mg/rat CD and BNF compared with control saline and BNF. (*B*) Alveolar macrophages cell count was significantly higher in all groups exposed to CD and BNF compared with the control saline with BNF. (*C*) AM CL was significantly higher in rats exposed to 40 mg CD and BNF compared with control saline and BNF. (*D*) NO-dependent AM CL was also significantly increased in rats exposed to 40 mg CD and BNF compared with control saline and BNF. (*E*) CD and BNF exposure causes a dose-dependent increase in LDH that indicates pulmonary cytotoxicity ($r^2 = 0.963$, $P = 0.003$). (*F*) CD and BNF increased BAL albumin in rats exposed to 20 mg and 40 mg/rat CD compared with BNF alone indicating pulmonary vascular damage. The *bars* are values of means and SE for each treatment. *Significantly different from control group at $P < 0.05$.

Discussion

Some epidemiologic studies report that coal miners, primarily smokers, have a lower risk of developing lung cancer compared with control nonminers (43). Moreover, lung cancer risk in workers exposed to the more toxic particles, such as silica, was mostly absent when workers were concurrently exposed to other workplace lung carcinogens, such as PAHs (44). Such data concerning lung cancer in miners are difficult to interpret because miners are exposed to a mixture of environmental pollutants; such as the CD particles and the PAHs in cigarette smoke.

Using rats with induced CYP1A1, as it is in cigarette smokers, EROD data show that CD exposure suppressed induced CYP1A1 activity in a dose-dependent fashion. However, the dose dependency of the suppressed EROD induction does not imply that the response is linear, only that it follows the basic assumptions of dose–response relationships (45). Indeed the suppression of EROD induction is the result of the administration of respirable CD, the magnitude of the EROD suppression is dependent upon the dose of the coal, and EROD activity is readily quantifiable. Thus, the basic assumptions of dose-responsiveness are met and there is statistically significant association between increasing concentrations of administered CD and the suppression of BNF-induced EROD activity ($P = 0.0028$, linear regression). However, the linear regression analysis also indicates that the data fit a straight line poorly ($r^2 = 0.399$). Indeed, only the 20 and 40 mg CD exposures significantly suppressed BNF-induced EROD activity, which suggests that the response may be complex.

Previous studies in our laboratory show that intratracheal

exposure of rat lungs to crystalline silica (20 mg/rat) significantly suppressed induced EROD activity (23). Although CD is less cytotoxic than silica (9), it is able to inhibit the CYP1A1-dependent enzymatic activity (EROD) in a dose-responsive manner, suggesting that CD particles, like silica, can interfere with CYP1A1 metabolic activity in rat lungs. Western blot analysis was performed, using a polyclonal rabbit anti-rat CYP1A1 antibody to detect CYP1A1 protein expression in the lung microsomes. The amount of CYP1A1 protein in the gel was reduced at all doses of CD treatment, but was significant only at the highest dose (40 mg/rat). This suggests that the reduction in the CYP1A1 activity upon exposure to CD is partly attributed to the reduction of CYP1A1 expression and protein synthesis by different pulmonary cells.

The activity of CYP2B1, measured in lung microsomes as PROD activity, showed a dose-dependent suppression by exposure to CD. The suppression of PROD by CD again fulfills the basic assumption of a dose–response (45). The suppression of PROD activity is the result of the administration of respirable CD, the magnitude of the PROD suppression is dependent upon the dose of the coal, and PROD activity is readily quantifiable. Increasing concentrations of CD are highly significantly associated with suppression of PROD activity ($P = 0.001$, linear regression) but do not fit a straight line well ($r^2 = 0.458$, linear regression). This suggests a response that is more complex than a simple linear response. The suppression of PROD activity by CD is similar to the suppression of PROD activity noted in the lungs of rats exposed to diesel or carbon black particles (20).

CYP2B1 is the major constitutive isoform of CYPs in rat lungs (46, 47). CYP2B1 expression is not inducible in the rat lung (46). BNF, a specific CYP1A1 inducer, significantly upregulates CYP1A1 expression in the lung parenchyma (25, 48, 49). Western blot analysis for CYP2B1 showed a reduction of the protein, albeit not significant, in BNF plus CD-exposed rats compared with rats receiving BNF alone. Together, these data suggest that CD exposure modified not only the CYP1A1 expression and activity but also the activity of CYP2B1 in the rat lung.

Cell-specific expression and localization of CYP1A1 were studied by immunofluorescence followed by quantification, using morphometric analysis. Immunofluorescence was employed in this study because it was more sensitive than enzymatic immunohistochemistry and useful for localizing the sites of pulmonary CYP1A1 through double labeling (50). Morphometric analysis of immunofluorescent-stained sections for CYP1A1 demonstrated that within the alveolar septum, CYP1A1 expression area was generally localized to flattened cells morphologically consistent with type I pneumocytes but expression by other flattened septal cells, such as endothelial cells, could not be excluded. Using colocalization to sites of cytokeratins 8/18 expression to determine AT-II CYP1A1 expression, it was demonstrated that most of the alveolar area expressing CYP1A1 was not occupied by AT-II. This was not surprising because alveolar type I epithelial cells cover $> 90\%$ of the internal surface area of the lungs (51, 52), whereas AT-II account for $< 10\%$ (53). Moreover, it has been observed by *in situ* hybridization in the lungs of 3-methylcholanthere–induced rats that CYP1A1 labeling was visualized in other alveolar wall cells that could be either capillary endothelial cells or alveolar type I pneumocytes (54). An overall reduction of CYP1A1 expression within the alveolar septum was observed in BNF-induced rats exposed to 20 mg and 40 mg CD/rat compared with those exposed to BNF induction plus saline. These results were consistent with EROD activity, suggesting that both CYP1A1 protein expression in the alveolar septum and its metabolic function throughout the lung are suppressed by CD exposure. Localization of CYP1A1 in terminal nonciliated bronchiolar epithelial (Clara) cells was also investigated. Clara cells are considered the major area of CYP1A1 expression in lungs because they are rich in agranular endoplasmic reticulum where CYP1A1 is localized (55). The number of CYP1A1-positive cells was counted per micrometer of the basement membrane. This number did not show a significant change in rats exposed to CD plus BNF compared with the BNF control. This result suggested that CD modified CYP1A1 expression at the alveolar rather than the bronchiolar level, presumably because the CD particles tend to aggregate in alveolar regions adjacent to the alveolar duct.

Histopathologic changes assessed in stained sections showed that CD exposure enhanced the pulmonary inflammatory response. Lung inflammation was characterized by intra-alveolar and interstitial accumulation of macrophages and rare neutrophils. The dust-laden macrophages were enlarged and often aggregated in clumps of two or more cells. The alveolar inflammation was often centered around alveolar ducts where CD particles were deposited. BAL fluid contained increased numbers of macrophages in all CD-exposed rats. Increased numbers of BAL neutrophils were seen in BAL of rats exposed to 10, 20, or 40 mg CD. Thus, lung inflammation was present and confirmed by two different techniques. These findings were consistent with those previously described in rats inhaling 50 mg/m^3 CD for 32 d or 10 mg/m^3 CD for 52 d (56). Aggregates of dust-laden macrophages and the appearance of cuboidal (hypertrophied) alveolar epithelial cells has been previously observed in rats inhaling 1.97 mg/m^3 respirable CD 7 h/d, 5 d/wk for 3–12 mo (19).

Previous studies suggest that inflammation can inhibit CYP activity. For example, the ability of the liver to metabolize drugs in rodents is impaired after inflammatory stimuli that are accompanied by a depletion of total hepatic CYP content and a declined microsomal metabolism of drug substrates (57, 58). In other similar studies, the experimentally-induced inflammatory reactions resulted in a reduction of the microsomal CYP concentration and their metabolizing activity in the liver (59–62). In addition, exposure of cultured hepatocytes to inflammatory stimuli decreased the total microsomal CYP, CYP-catalyzed enzyme activities, and levels of CYP proteins and mRNAs (63). *In vivo* induction of interferon α/β in BNF-exposed rats results in both reduced CYP1A1 gene transcription and increased CYP1A1 mRNA degradation in liver cells (21). For CYP1A1, tumor necrosis factor-α and lipopolysaccharide markedly inhibit the induction of CYP1A1 by 2,3,7,8-tetrachlorodibenzo-*p*-dioxin (22). Inflammation-associated inhibition of CYP1A1 induction appears to involve inhibition of acetylation of the CYP1A1 promoter by tumor necrosis factor-α, and involves nuclear factor-κB (22). In addition, nitric oxide can be produced during pulmonary inflammation (64) and directly inhibits CYP1A1 activity *in vitro* in Chinese hamster cells (65). Although relatively little data describe the effect of inflammation on extrahepatic CYP expression, some evidence suggests that extrahepatic CYPs are likely to be differentially regulated by different inflammatory stimuli (66). The CD-induced pulmonary inflammation shown in the current experiment was associated with suppression of pulmonary CYP1A1 induction and CYP2B1 activity in the rats. Studies of possible roles of proinflammatory mediators are underway. Importantly, in our study, CYP1A1 and CYP2B1 activities were only significantly decreased by exposures that also produced significant cytoxicity and protein leakage in the lung, as assessed by LDH and albumin release into the BAL.

After lung injury at the alveolar level, the damage of type I pneumocytes is repaired by progenitor AT-II that can proliferate and regenerate the damaged alveolar surface and may differentiate into type I pneumocytes thus reconstituting the alveolar architecture (52, 67). The hypertrophy and hyperplasia of AT-II

were obvious in immunofluorescence and histopathology. Despite the increasing numbers (hyperplasia) and size (hypertrophy) of AT-II, AT-II–specific CYP1A1 expression decreased as many of these cells were devoid of detectable CYP1A1. This suggested that CD exposure was associated with the appearance of new populations of AT-II but that many of these cells did not contain detectable amounts of CYP1A1. A number of investigators have reported that CYP activities and the level of CYP apoproteins decreased after partial hepatectomy and regeneration of hepatic cells (68–71). The priority of hepatic cell function during regeneration is the key factor where the replication, but not the transcription, is the main function of DNA regenerating the cells (72–75). Consistent with that were the higher levels of CYP2B1 protein expression and mRNA in freshly isolated AT-II cells, but these levels diminished in the cell culture (76). One possible explanation for our findings may be that like regenerating hepatocytes, AT-II during the hyperplasia and hypertrophy, are mainly devoted to proliferation and not to expressing CYP1A1. Previous morphometric studies demonstrated that the alveolar tissue represents 87% of the total lung volume in rats where the volume of type I cells is more than twice that of AT-II (77). Thus, the loss of type I cells and their replacement by a hypertrophied and hyperplastic population of AT-II cells with diminished CYP1A1 expression may be one mechanism of decreased CYP1A1 induction in CD exposure. Additional studies will be needed to determine the effect of chronic CD exposure on CYP1A1 induction and constituitive CYP2B1 expression.

In conclusion, our data show for the first time that CD exposure had a modifying effect on the BNF-induced CYP1A1 expression and altered its cell-specific localization in the rat lung. CD was able to suppress the activity and expression of CYP1A1 as demonstrated by the dose-dependent reduction of EROD activity and diminution of CYP1A1 apoprotein measured by Western blot analysis. Not only was CYP1A1 induction modified by CD exposure, but the activity of another CYP isoform, CYP2B1, was suppressed in a dose-dependent fashion. The overall results suggested that CD exposure had the ability to trigger pulmonary inflammation and was a complex modifier of CYP1A1 induction in rat lungs.

Acknowledgments: The authors gratefully acknowledge the expert assistance of Lyndell Millecchia for photomicroscopy and Diane Schwegler-Berry and Patsy Willard for excellent technical assistance. Appreciation is extended to Mike Whitmer for the endotoxin analysis of the instilled CD suspension. This manuscript represents a portion of the dissertation research of M.G., which was submitted to West Virginia University in partial fulfillment of the degree of Doctor of Philosophy. This research was supported by as an intramural project (39277263) of the National Institute for Occupational Safety and Health. A research stipend was funded in part by the Advanced Research Foundation Inc.

References

1. Whitlock, J. P., Jr. 1999. Induction of cytochrome P4501A1. *Ann. Rev. Pharm. Toxicol.* 39:103–125.
2. Hasler, J. A., R. Estabrook, M. Murray, I. Pikuleva, M. Waterman, J. Cappdevila, V. Holla, C. Helvig, J. R. Falck, G. Farrell, L. S. Kaminsky, S. D. Spivack, E. Boitier, and P. Beaune. 1999. Human cytochrome P450. *Mol. Aspects Med.* 20:1–137.
3. Crespi, C. L., R. Langenbach, K. Rudo, Y. T. Chem, and R. L. Davies. 1989. Transfection of human cytochrome p-450 into the human lymphoblastiod cell line, AHH-1, and use of the recombinant cell line in gene mutation assays. *Carcinogen* 10:295–301.
4. Eaton, D. L., E. P. Gallagher, T. K. Bammler, and K. L. Kunze. 1995. Role of cytochrome P4501A2 in chemical carcinogenesis: Implications for human variability in expression and enzyme activity. *Pharmacogen.* 5:259–274.
5. Shimada, T., M. Iwasaki, M. V. Martin, and F. P. Guengerich. 1989. Human liver microsomal cytochrome P-450 enzymes involved in the bioactivation of procarcinogens detected by Umu gene response in *Salmonella typhimurium* TA 1535/pSK1002. *Cancer Res.* 12:3218–3228.
6. Ma, Q., and J. P. Whitlock, Jr. 1997. A novel cytoplasmic protein that interacts with the Ah receptor contains tetratricopeptide repeat motifs, and augments the transcriptional response to 2,3,7,8-tetrachlorodibenzo p-dioxin. *J. Biol. Chem.* 272:8878–8884.
7. Tian, Y., S. Ke, M. S. Denison, A. B. Rabson, and M. A. Gallo. 1999. Ah receptor and NF-κB interactions, a potential mechanism for dioxin toxicity. *J. Biol. Chem.* 274:510–515.
8. Sorenson, J. R. J., T. E. Kober, and H. G. Petering. 1974. The concentration of Cd, Cu, Fe, Ni, Pb, and Zn in bituminous coal from mines with differing incidences of coal workers' pneumoconiosis. *Am. Ind. Hyg. Assoc. J.* 25: 93–98.
9. Castranova, V. 2000. From coal mine dust to quartz: mechanisms of pulmonary pathogenecity. *Inhal. Toxicol.* 12:7–14.
10. Kuempel, E. D., E. J. O'Flaherty, L. T. Stayner, R. J. Smith, F. H. Y. Green, and V. Vallyathan. 2001. A biomathematical model of particle clearance and retention in the lungs of coal miners. *Regul. Toxicol. Pharmacol.* 34:69–87.
11. Douglas, A. N., A. Robertson, J. S. Chapman, and V. A. Ruckley. 1986. Dust exposure, dust recovered from the lung, and associated pathology in a group of British coalminers. *Br. J. Ind. Med.* 43:795–801.
12. Rom, W. N., P. B. Bitterman, S. I. Rennard, A. Cantin, and R. G. Crystal. 1987. Characterization of the lower respiratory tract inflammation of nonsmoking individuals with interstitial lung disease associated with chronic inhalation of inorganic dusts. *Am. Rev. Respir. Dis.* 136:1429–1434.
13. Kuempel, E. D., M. D. Attfield, V. Vallyathan, N. L. Lapp, J. M. Hale, R. J. Smith, and V. Castranova. 2003. Pulmonary inflammation and crystalline silica in respirable coal mine dust: dose response. *J. Biosci.* 28:61–79.
14. Kuempel, E. D., L. T. Stayner, M. D. Attfield, and C. R. Buncher. 1995. Exposure response analysis of mortality among coal miners in United States. *Am. J. Ind. Med.* 28:167–184.
15. Meijers, J. M. M., G. M. H. Swaen, J. J. M. Slangen, K. van Vliet, and F. Sturmans. 1991. Long term mortality in miners with coal workers' pneumoconiosis in Netherlands: a pilot study. *Am. J. Ind. Med.* 19:43–50.
16. Alexandrov, K., I. Cascorbi, M. Rojas, G. Bouvier, E. Kriek, and H. Bartsch. 2002. CYP1A1 and GSTM1 genotypes affect benzo(a)pyene DNA adducts in smokers' lung: comparison with aromatic/hydrophobic adduct formation. *Carcinogenesis* 23:1969–1977.
17. Miles, P. R., L. Bowman, and M. R. Miller. 1993. Alterations in the pulmonary microsomal cytochrome P-450 system after exposure of rats to silica. *Am. J. Respir. Cell Mol. Biol.* 8:597–604.
18. Miles, P. R., L. Bowman, W. G. Jones, D. S. Berry, and V. Vallyathan. 1994. Changes in alveolar lavage material and lung microsomal xenobiotic metabolism following exposures to HCl-washed or unwashed crystalline silica. *Toxicol. Appl. Pharmacol.* 129:235–242.
19. Green, F. H. Y., R. L. Boyd, J. Danner-Rabovsky, M. J. Fisher, W. J. Moorman, T.-M. Ong, J. Tucker, V. Vallyathan, W.-Z. Whong, J. Zoldak, and T. Lewis. 1983. Inhalation studies of diesel exhaust and coal dust in rats. *Scand. J. Work Environ. Health* 9:181–188.
20. Rengasamy, A., M. W. Barger, E. Kane, J. K. Ma, V. Castranova, and J. Y. Ma. 2003. Diesel exhaust particle-induced alterations of pulmonary phase I and phase II enzymes of rats. *J. Toxicol. Environ. Health A* 66:153–167.
21. Delaporte, E., and K. W. Renton. 1997. Cytochrome P4501A1 and cytochrome P4501A2 are downregulated at both transcriptional and post-transcriptional levels by conditions resulting in interferon-α/β induction. *Life Sci.* 60:787–796.
22. Ke, S., A. B. Rabson, J. F. Germino, M. A. Gallo, and Y. Tian. 2001. Mechanism of suppression of cytochrome P-450 1A1 expression by tumor necrosis factor-α and lipopolysaccharide. *J. Biol. Chem.* 276:39638–39644.
23. Battelli, L. A., A. F. Hubbs, R. D. Simoskevitz, V. Vallyathan, L. Bowman, and P. R. Miles. 1999. Cytochrome P450 1A1 and 2B1 in rat lung: exposure to silica and inducers of xenobiotic metabolism. *Toxicol. Sci.* 48:S97. (Abstr.)
24. Levy, R. D., A. F. Hubbs, B. S. Ducatman, G. Singh, V. Vallyathan, L. Bowman, and P. R. Miles. 1997. Metabolic functions of alveolar type II cells in acute silicosis. *Fund. Appl. Toxicol.* 36:S74. (Abstr.)
25. Lee, C., K. C. Watt, A.-M. Chang, C. G. Plopper, A. R. Buckpitt, and K. E. Pinkerton. 1998. Site-selective differences in cytochrome P450 isoform activities: comparison of expression in rat and Rhesus monkey lung and induction in rats. *Drug Metab. Dispos.* 26:396–400.
26. Vallyathan, V., D. Schwegler, M. Reasor, L. Stettler, J. Clere, and F. H. Y. Green. 1988. Comparative in vitro cytotoxicity and relative pathogenicity of mineral dusts. *Ann. Occup. Hyg.* 32:S279–S289.
27. Porter, D. W., A. F. Hubbs, V. A. Robinson, L. A. Battelli, M. Greskevitch, M. Barger, D. Landsittel, W. Jones, and V. Castranova. 2002. Comparative pulmonary toxicity of blasting sand and five substitute abrasive blasting agents. *J. Toxicol. Environ. Health A* 65:1121–1140.
28. Driscoll, K. E., D. L. Costa, G. Hatch, R. Henderson, G. Oberdorster, H. Salem, and R. B. Schlesinger. 2000. Intratratracheal instillation as an exposure technique for the evaluation of respiratory tract toxicity: uses and limitation. *Toxicol. Sci.* 55:24–35.
29. Flowers, N. L., and P. R. Miles. 1991. Alterations of pulmonary benzo[a]pyrene metabolism by reactive oxygen metabolites. *Toxicol.* 68:259–274.
30. Ma, J. Y. C., H. M. Yang, M. W. Barger, P. D. Siegel, B. Z. Zhong, A. J. Kriech, and V. Castranova. 2002. Alteration of pulmonary cytochrome P-450 system: effects of asphalt fume condensate exposure. *J. Toxicol. Environ. Health A* 65:101–104.
31. Smith, P. K., R. I. Krohn, G. T. Hermanson, A. K. Mallia, F. H. Gartner, M. D. Provenzano, E. K. Fujimoto, N. M. Goeke, B. J. Olson, and D. C. Klenk. 1985. Measurement of protein using bicinchoninic acid. *Anal. Biochem.* 150:76–85.
32. Burke, M. D., S. Thompson, C. R. Elcombe, J. Halpert, T. Haaparanta, and R. T. Mayer. 1985. Ethoxy-, pentoxy-, and benzyloxyphenoxazones and

homologues: a series of substrates to distinguish between different induced cytochromes p-450. *J. Biol. Chem.* 34:3337–3345.
33. Kasper, M., T. Rudolf, A. A. Verhofstad, D. Schuh, and M. Muller. 1993. Heterogeneity in the immunolocalization of cytokeratin-specific monoclonal antibodies in the rat lung: evaluation of three different alveolar epithelial types. *Histochemistry* 100:65–71.
34. Nikula, K. J., K. J. Avila, W. C. Griffith, and J. L. Mauderly. 1997. Sites of particle retention and lung tissue responses to chronically inhaled diesel exhaust and coal dust in rats and cynomolgus monkeys. *Environ. Health Perspect.* 105:S(5)1231–S(5)1234.
35. Hubbs, A. F., V. Castranova, J. Y. C. Ma, D. G. Frazer, P. D. Siegel, B. S. Ducatman, A. Grote, D. Schwegler-Berry, V. A. Robinson, C. Van Dyke, M. Barger, J. Xiang, and J. Parker. 1997. Acute lung injury induced by a commercial leather conditioner. *Toxicol. Appl. Pharmacol.* 134:37–46.
36. Hubbs, A. F., N. S. Minhas, W. Jones, M. Greskevitch, L. A. Battelli, D. W. Porter, W. T. Goldsmith, D. Frazer, D. P. Landsittel, J. Y. Ma, M. Barger, K. Hill, D. Schwegler-Berry, V. A. Robinson, and V. Castranova. 2001. Comparative pulmonary toxicity of 6 abrasive blasting agents. *Toxicol. Sci.* 61:135–143.
37. Castranova, V., T. A. Jones, M. W. Barger, A. Afshari, and D. G. Frazer. 1990. Pulmonary responses of guinea pigs to consecutive exposures to cotton dust. *In* Proceedings of the 14th Cotton Dust Research Conference. R. R. Jacobs, P. J. Wakely and L. N. Domelsmith, editors. National Cotton Council, Memphis. 131–135.
38. Doumas, B., W. Watson, and H. Biggs. 1971. Albumin standards and the measurement of serum albumin with bromcresol green. *Clin. Chim. Acta* 31: 87–96.
39. Gay, R. J., R. B. McComb, and G. N. Bowers. 1968. Optimum reaction conditions for human lactate dehydrogenas isoenzymes as they affect total lactate dehydrogenase activity. *Clin. Chem.* 14:740–753.
40. Castranova, V., P. Lee, J. Y. C. Ma, K. C. Weber, W. H. Pailes, and P. R. Miles. 1987. Chemiluminescence from macrophages and monocytes. *In* Cellular Chemiluminescence. K. Van Dyke and V. Castranova, editors. CRC Press, Boca Raton. 4–19.
41. Hill, H. R., N. A. Hogan, J. F. Bale, and V. G. Hemming. 1977. Evaluation of nonspecific (alternative pathway) opsonic activity by neutrophil chemiluminescence. *Int. Arch. Allergy Appl. Immunol.* 53:490–497.
42. Allen, R. C. 1977. Evaluation of serum opsonic capacity by quantitating the initial chemiluminescent response from phagocytizing polymorphonuclear leukocytes. *Infect. Immun.* 15:828–833.
43. Costello, J., C. E. Ortmeyer, and W. K. C. Morgan. 1974. Mortality from lung cancer in US coal miners. *Amer. J. of Publ. Health* 64:222–224.
44. Cocco, P., C. H. Rice, J. Q. Chen, M. A. McCawley, J. K. McLaughlin, and M. Dosemeci. 2001. Lung cancer risk, silica exposure, and silicosis in Chinese mines and pottery factories: the modifying role of other workplace lung carcinogens. *Am. J. Ind. Med.* 40:674–682.
45. Eaton, D. L., and C. D. Klaassen. 2001. Principles of toxicology. *In* Casarett & Doull's Toxicology: The Basic Science of Poisons, Sixth Edition. C. D. Klaassen, editor. McGraw-Hill, New York. 11–34.
46. Guengerich, F. P., P. Wang, and N. K. Davidson. 1982. Estimation of isozymes of microsomal cytochrome P-450 in rats, rabbits, and human using immunochemical staining coupled with sodium dodecyl sulphate-polyacrimalide gel electrophoresis. *Biochemistry* 21:1698–1706.
47. Martin, J., D. Dinsdale, and I. N. White. 1993. Characterization of Clara and type II cells isolated from rat lung by fluorescence-activated flow cytometry. *Biochem. J.* 295:73–80.
48. Jones, K. G., J. F. Holland, G. L. Foureman, J. R. Bend, and J. R. Fouts. 1983. Xenobiotic metabolism in Clara cells and alveolar type II cells isolated from lungs of rats treated with β-naphthflavone. *J. Pharmacol. Exp. Ther.* 225:316–319.
49. Sesardic, D., K. J. Cole, R. J. Edwards, D. S. Davies, P. E. Thomas, W. Levin, and A. R. Boobis. 1990. The inducibility and catalytic activity of cytochromes P450c (P450IA1) and P450d (P450IA2) in rat tissues. *Biochem. Pharmacol.* 39:499–506.
50. Battelli, L. A., A. F. Hubbs, J. Y. Ma, M. L. Kashon, and V. Castranova. 2001. Quantifying cellular expression of cytochrome P-4501A1 (CYP1A1) in the pulmonary alveolus: a comparison of indirect enzymatic immunohistochemistry (IH) and indirect immunofluorescence (IF). *Toxicol. Sci.* 60:S403. (Abstr.)
51. Gonzalez, R. F., and L. G. Dobbs. 1998. Purification and analysis of RTI40, a type I alveolar epithelial cell apical membrane protein. *Biochim. Biophys. Acta* 1429:208–216.
52. Wang, H. C., C. T. Shun, S. M. Hsu, S. H. Kuo, K. T. Luh, and P. C. Yang. 2002. Fas/Fas ligand pathway is involved in the resolution of type II pneumocyte hyperplasia after acute lung injury: evidence from a rat model. *Crit. Care Med.* 30:1528–1534.
53. Castranova, V., J. Rabovsky, J. H. Tucker, and P. R. Miles. 1988. The alveolar type II epithelial cell: a multifunctional pneumocyte. *Toxicol. Appl. Pharmacol.* 93:472–483.
54. Pairon, J. C., N. Trabelsi, A. Buard, J. Fleury-Feith, C. M. Bachelet, F. Poron, P. Beaune, P. Brochard, and P. Laurent. 1994. Cell localization and regulation of expression of cytochrome P450 1A1 and 2B1 in rat lung after induction with 3-methylcholanthrene using mRNA hybridization and immunohistochemistry. *Am. J. Respir. Cell Mol. Biol.* 11:386–396.
55. Plopper, C. G. 1983. Comparative morphologic features of bronchiolar epithelial cells: the Clara cell. *Am. Rev. Respir. Dis.* 128:S37–S41.
56. Donaldson, K., G. M. Brown, D. M. Brown, M. D. Robertson, J. Slight, H. Cowie, A. D. Jones, R. E. Bolton, and J. M. Davis. 1990. Contrasting bronchoalveolar leukocyte responses in rats inhaling coal mine dust, quartz, or titanium dioxide: effects of coal rank, airborne mass concentration, and cessation of exposure. *Environ. Res.* 52:62–76.
57. Bissell, D. M., and L. E. Hammaker. 1976. Cytochrome P-450 heme and the regulation of hepatic heme oxygenase activity. *Arch. Biochem. Biophys.* 176:91–102.
58. Ghezzi, P., B. Saccardo, P. Villa, V. Rossi, M. Bianchi, and C. A. Dinarello. 1986. Role of interleukin-1 in the depression of liver drug metabolism by endotoxin. *Infect. Immun.* 54:837–840.
59. Beck, F. J., and M. W. Whitehouse. 1974. Impaired drug metabolism in rats associated with acute inflammation: a possible assay for anti-injury agents. *Proc. Soc. Exp. Biol. Med.* 145:135–140.
60. Baer, A. N., and F. A. Green. 1989. Cytochrome P-450 mediated-metabolism in active murine systemic lupus erythematosus. *J. Rheumatol.* 16:335–338.
61. Endo, Y., S. Tsuriya, and E. Fujihira. 1981. Hepatic drug-metabolizing activities and anti-inflammatory potency of hydrocortisone in rats with granulatomous inflammation. *Res. Commun. Chem. Pathol. Pharmacol.* 33:195–206.
62. Mahu, J. L., and G. Feldmann. 1984. Study of biochemical behavior of some exported and nonexported hepatic protein during an acute inflammatory reaction in the rat. *Enzyme* 31:234–240.
63. Morgan, E. T. 1997. Regulation of cytochromes P450 during inflammation and infection. *Drug Metab. Rev.* 29:1129–1188.
64. Porter, D. W., L. Millecchia, V. A. Robinson, A. Hubbs, P. Willard, D. Pack, D. Ramsey, J. McLaurin, A. Khan, D. Landsittel, A. Teass, and V. Castranova. 2002. Enhanced nitric oxide and reactive oxygen species production and damage after inhalation of silica. *Am. J. Physiol. Lung Cell. Mol. Physiol.* 283:L485–L493.
65. Stadler, J., J. Trockfeld, W. A. Schmalix, T. Brill, J. R. Siewert, H. Greim, and J. Doehmer. 1994. Inhibition of cytochromes P4501A by nitric oxide. *Proc. Natl. Acad. Sci. USA* 91:3559–3563.
66. Morgan, E. T. 2001. Regulation of cytochrome P450 by inflammatory mediators: why and how? *Drug Metab. Dispos.* 29:207–212
67. Melloni, B., O. Lesur, A. Cantin, and R. Begin. 1993. Silica-exposed macrophages release a growth-promoting activity for type II pneumocytes. *J. Leukoc. Biol.* 53:327–335.
68. Hino, Y., Y. Imai, and R. Sato. 1974. Induction by phenobarbital of hepatic microsomal drug-metabolizing enzyme system in partially hepatectomized rats. *J. Biochem. (Tokyo)* 76:735–744.
69. Klinger, W., and E. Karge. 1987. Interaction of induction, ontogenic development and liver regeneration on the monooxygenase level. *Exp. Pathol.* 31: 117–124.
70. Presta, M., M. G. Aletti, and G. Ragnotti. 1980. Decrease of the activity of the mixed function oxidase system in regenerating rat liver: an alternative explanation. *Biochim. Biophys. Res. Commun.* 95:829–834.
71. Ronis, M. J. J., C. K. Lumpkin, P. E. Thomas, M. Ingelman-Sundberg, and T. M. Badger. 1992. The microsomal monooxygenase system of regenerating liver. *Biochem. Pharmacol.* 43:567–573.
72. Liddle, C., M. Murray, and G. C. Farrell. 1989. Effect of liver regeneration on hepatic cytochrome P450 isozymes and serum sex steroids in the male rat. *Gastroenterol.* 96:864–872.
73. Morgan, E. T., C. MacGeoch, and J. A. Gustafsson. 1985. Hormonal and Developmental regulation of the expression of the hepatic microsomal steroid 16α-hydroxylase cytochrome P450 apoprotein in the rat. *J. Biol. Chem.* 260:11895–11898.
74. Steer, C. J. 1995. Liver regeneration. *FASEB J.* 9:1396–1400.
75. Waxman, D. J. 1989. Hepatic enzymes of steroid metabolism. Regulation of growth hormone secretory patterns. *In* Cytochrome P 450: Biochemistry and Biophysics. I. Schuster, editor. Taylor and Francis, London. 464–471.
76. Lag, M., R. Becher, J. T. Samuelsen, R. Wiger, M. Refsnes, H. S. Huitfeldt, and P. E. Schwarze. 1996. Expression of CYP2B1 in freshly isolated and proliferating cultures of epithelial rat lung cells. *Exp. Lung Res.* 22:627–649.
77. Crapo, J. D., S. L. Young, E. K. Fram, K. E. Pinkerton, B. E. Barry, and R. O. Crapo. 1983. Morphometric characteristic of cells in the alveolar region of mammalian lungs. *Am. Rev. Respir. Dis.* 128:S42–S46.